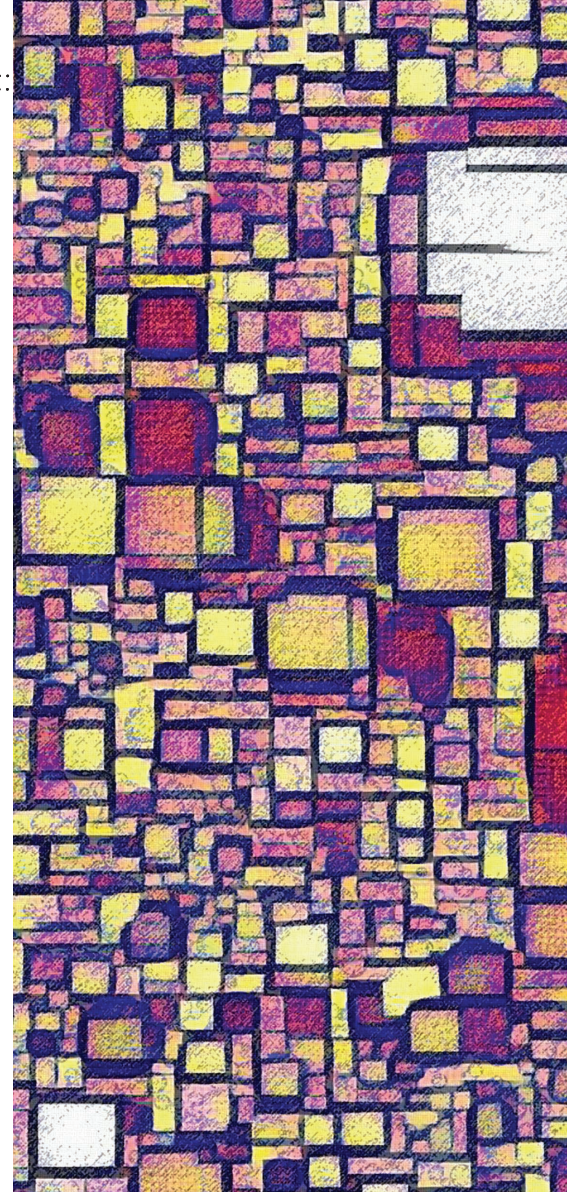


A Review of Change Detection in Multitemporal Hyperspectral Images

Current techniques, applications, and challenges

SICONG LIU, DANIELE MARINELLI, LORENZO BRUZZONE,
AND FRANCESCA BOVOLO



The expected increasing availability of remote sensing satellite hyperspectral (HS) images provides an important and unique data source for Earth observation (EO). HS images are characterized by a detailed spectral sampling (i.e., very high spectral resolution) over a wide spectral wavelength range, which makes it possible to monitor land-cover dynamics at a fine spectral scale. This is due to its capability of detecting subtle spectral variations in multitemporal images associated with land-cover changes that are not detectable in traditional multispectral (MS) images because of their limited spectral resolution (i.e., sufficient for representing only abrupt, strong changes in the spectral signature, as a rule). To fully exploit the available multitemporal HS images and their rich information content in change detection (CD), it is necessary to develop advanced automatic techniques that can address the complexity of the extraction of change information in an HS space. This article provides a comprehensive overview of the CD prob-

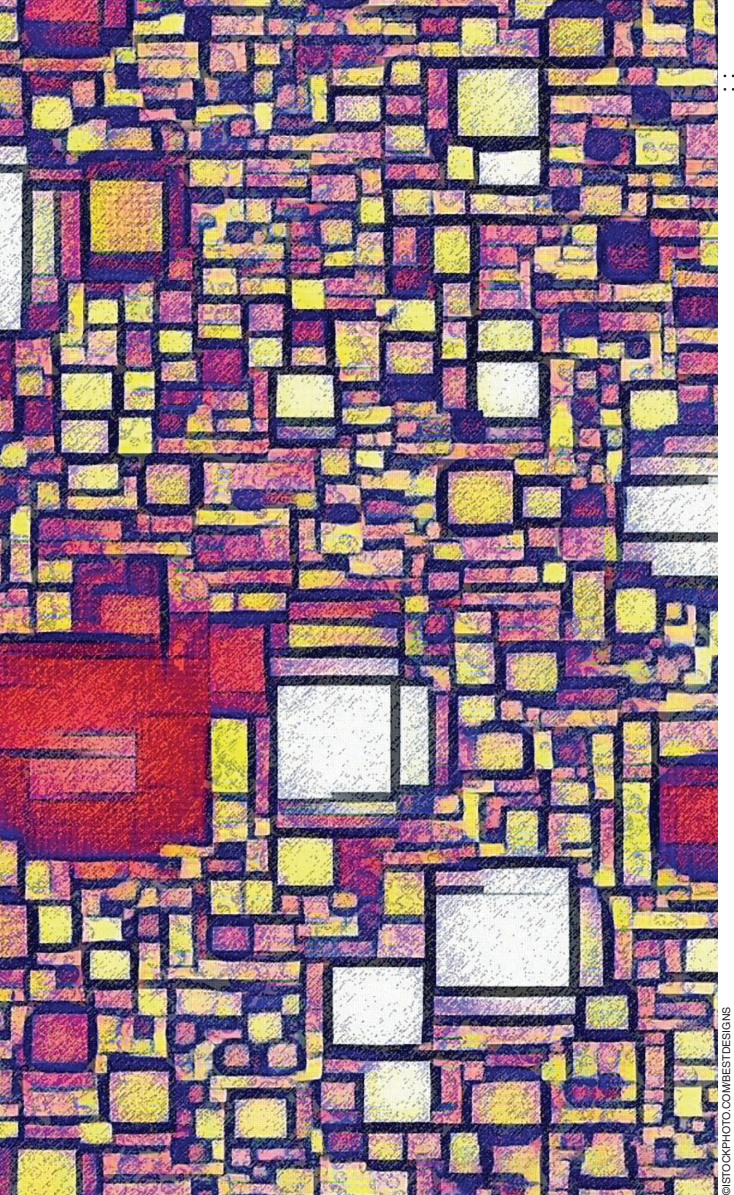
lem in HS images, as well as a survey on the main CD techniques available for multitemporal HS images. We review both widely used methods and new techniques proposed in the recent literature. The basic concepts, categories, open issues, and challenges related to CD in HS images are discussed and analyzed in detail. Experimental results obtained using state-of-the-art approaches are shown, to illustrate relevant concepts and problems.

BACKGROUND AND PURPOSE

Due to the revisit property of polar orbiting satellites, it is possible to acquire images over the same geographical area at multiple times. The use of remote sensing data acquired at different times to detect changes has proven to be a valuable tool in many applications related to monitoring the land surface dynamic.

To date, most remote sensing sensors mounted onboard satellites are MS and synthetic aperture radar (SAR) systems, thus making MS and SAR images the main data sources for EO applications [1]. In contrast, compared with available MS and SAR images, multitemporal HS image availability is

Digital Object Identifier 10.1109/MGRS.2019.2898520
Date of publication: 18 June 2019



©STOCKPHOTO.COM/BESTDESIGNS

still poor. After the NASA EO-1 satellite (mounted onboard the Hyperion HS sensor) was deactivated in March 2017 and the HS Imager for the Coastal Ocean failed because of a

solar storm in September 2014, few spaceborne sensors are still operating. Among them, there are the European Space Agency's compact high-resolution imaging spectrometer sensors mounted on the PROBA-1 satellite [2], the HS imager sensor mounted onboard the Chinese satellite *HJ-1B* [3], the HS imager mounted onboard the Indian *IMS-1* satellite [4], and the visual and infrared (IR) HS sensor mounted on the Chinese *Gaofeng-5* satellite launched on 9 May 2018. Therefore, there is limited availability of multitemporal HS data, which has led to limited development of ad hoc CD methods. However, the *Precursore Iperspettrale della Missione Applicativa* (PRISMA) [5] was launched on 21 March 2019 [85], and, in the near future, other satellite missions with HS sensors will follow, including

- ▷ HS Imager Suite (HISUI), planned for launch in 2019 [6]
- ▷ Environmental Mapping and Analysis Program (EnMAP), planned for launch in 2020 [7]
- ▷ HS IF Imager (HyspIRI), scheduled for launch after 2022 [8]
- ▷ Spaceborne HS Applicative Land and Ocean Mission (SHALOM), scheduled for launch after 2022 [9]
- ▷ HS X Imagery (HypXIM), scheduled for launch after 2023 [10].

Table 1 shows the main parameters of these HS future missions, which will significantly increase the availability of HS data, thus accelerating related scientific research and applications. Accordingly, HS images will become valuable data sources for EO and dynamic monitoring applications. However, the data distribution policy for these future HS missions is still unclear, which might limit their use.

CD techniques compare images acquired at different times to identify changes in land cover measured by the remote sensing sensors (e.g., reflected radiance for passive optical sensors). CD has been one of the most important remote sensing research activities (on methodologies and applications) in recent decades [11]. CD techniques have been developed and successfully used in different remote sensing applications, such as agriculture and forestry monitoring [12], [13], natural-disaster mapping [14], [15],

TABLE 1. THE MAIN PARAMETERS OF SOME FUTURE SPACEBORNE HS MISSIONS (PARAMETERS MAY CHANGE BEFORE LAUNCH).

PARAMETERS	PRISMA	HISUI	EnMAP	HyspIRI	SHALOM	HypXIM
Country	Italy	Japan	Germany	United States	Italy/Israel	France
Spectral range (nm)	VNIR SWIR	400–1,010 920–2,505	400–970 920–2,500	400–1,000 900–2,450	380–2,510	400–2,500
Spectral sampling (nm)	VNIR SWIR	≤12	10 12.5	6.5 10	10	10
Number of bands	VNIR SWIR	66 173	57 128	88 154	214	275
Swath width (km)		30	30	30	30	15
Spatial resolution (m)		30	30	30	10	8
Revisit time (days)		6	2–60	4–27	16	4
Planned launch year		2019	2019	2020	≥2022	≥2023

VNIR: visible-near IR; SWIR: short-wave IR.

and urban landscape and sprawl analysis [16]–[18]. Past CD research has focused mainly on the design of CD techniques in multitemporal MS and SAR images (with both moderate and high spatial resolutions) due to their large availability. Only a few studies have addressed CD in HS images. Due to the expected increase of multitemporal HS images, CD in multitemporal HS images will become one of the most interesting research and application directions in the future.

Most HS optical passive sensors measure the reflectance of a given object in the range from the visible ($0.4\text{--}0.7\ \mu\text{m}$) to the short-wave IR (i.e., up to approximately $2.5\ \mu\text{m}$). A given sensor may work only in a certain portion of this wavelength range. The sensor samples the reflected radiance at a given high spectral resolution (e.g., $10\ \text{nm}$). This dense sampling of the spectrum allows for a precise representation of the reflectance of each pixel, resulting in a fine measure of the spectral signature. An example of the

HS cube and pixel spectral signatures associated with different land-cover materials is shown in Figure 1. The spectral signatures of different materials have distinct spectral shapes that can be used to discriminate among them, even in terms of the subclasses within a general class (i.e., vegetation types).

Due to the coarse spectral sampling in a few discrete spectral bands of MS sensors, the early stage of the development of CD techniques for these images focuses mainly on the identification of strong, abrupt changes. Such land-cover changes present a significant variation of the spectral signatures (e.g., vegetation to built-up areas, water to soil). Taking advantage of the detailed spectral sampling of HS sensors, the aim of CD in HS images is to detect changes associated with large spectral variations as well as those related to minor variations of the spectrum (usually not detectable from MS images). These changes most often affect only some portions of the spectral signatures.

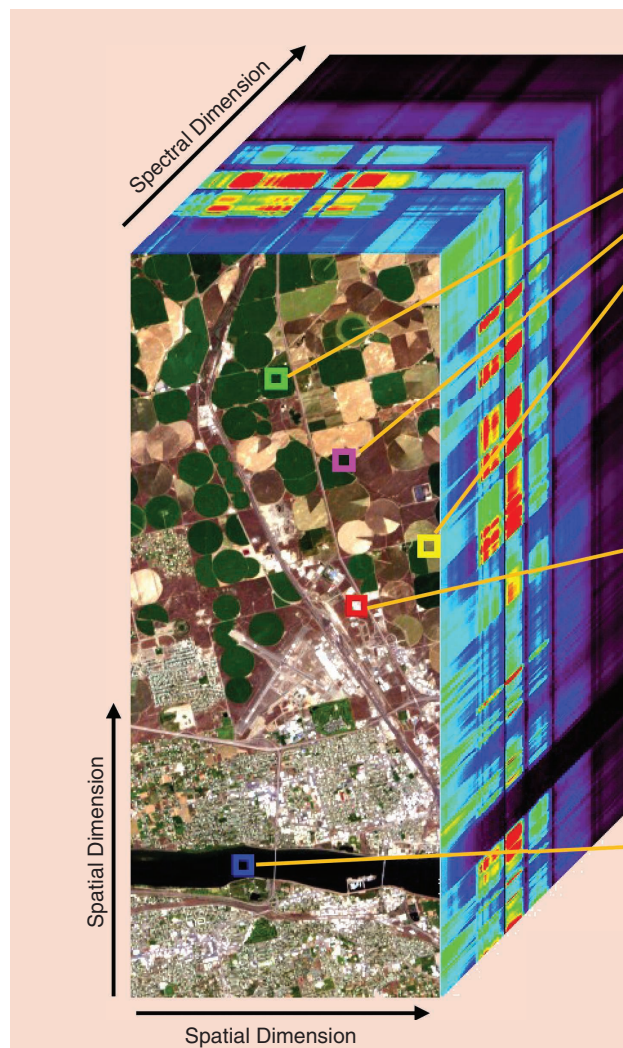


FIGURE 1. An example of an HS image cube for an agricultural area in Benton County, Washington (true color composite of EO1H0440282007128110PY Hyperion product, courtesy of the U.S. Geological Survey), and the pixel spectral signatures associated with different land-cover materials.

Thus, ad hoc techniques are required to identify these minor spectral variations in the spectral-temporal domain. In this article, we analyze the CD problem in HS images and present a comprehensive overview of the existing methods, including the most widely used and most recently published ones.

CATEGORIES OF CHANGE-DETECTION APPROACHES FOR HYPERSPECTRAL IMAGES

CD approaches can be grouped in several ways by considering different perspectives. In the literature, there are some excellent review articles that provide categorization of CD techniques [13], [19]–[21]. However, they focus mainly on MS images, and very few works (e.g., [22], [23]) provide a review of CD techniques in HS images.

In general, we can divide CD approaches in HS images by considering different possible variables (see Figure 2).

- 1) *Application purpose*: Four classes can be defined: anomalous, binary, multiclass, and time-series CD methods.
- 2) *Availability of ground reference data*: Three classes can be defined: supervised, semisupervised, and unsupervised CD methods.
- 3) *Automation degree*: Three classes can be defined: fully automatic, semiautomatic, and manual CD methods.

In this article, we use the first categorization because it is the most interesting from methodological and application perspectives. We performed an analysis on CD in HS images articles published in IEEE journals and conference

papers during the previous five years of our study (i.e., 2012–2017), as shown in Figure 3. This was accomplished by searching articles according to the keywords in the first category (i.e., *anomalous*, *binary*, *multiclass*, and *time-series CD*) jointly with the keyword “hyperspectral.” Then, a manual filtering was carried out by analyzing the title and context of each article. Relatively few articles on CD in HS images have been published compared with other hot topics in the HS field, such as classification and unmixing. Among them, in the past five years, the topic of anomalous CD (ACD) had the most published articles (25 out of 109). Multiclass CD and time-series CD were the topics of the second and third groups, with 16 and 13 articles, respectively. Binary CD was addressed in only seven articles. In addition, 48 articles focused on specific CD applications (e.g., cryosphere CD [24]) or could not be assigned to any of the categories. Figure 3 shows a pie chart representing the distribution of the articles according to our categorization.

RELATIVELY FEW ARTICLES ON CD IN HS IMAGES HAVE BEEN PUBLISHED COMPARED WITH OTHER HOT TOPICS IN THE HS FIELD, SUCH AS CLASSIFICATION AND UNMIXING.

CHANGE-DETECTION PROBLEM IN HYPERSPECTRAL IMAGES

CD is a systematic process that requires a series of comprehensive processing steps, which include [20], [25] 1) understanding the CD problem, 2) selecting suitable remote sensing data, 3) accurate image preprocessing, 4) selecting suitable features, 5) designing the CD algorithm, and 6) evaluating the CD performance. In each step, significant effort should be aimed at defining successful procedures to obtain high-quality data input through the CD technique and then a high-accuracy CD output. If we consider the CD problem in a pair of bitemporal HS images, we can define the block

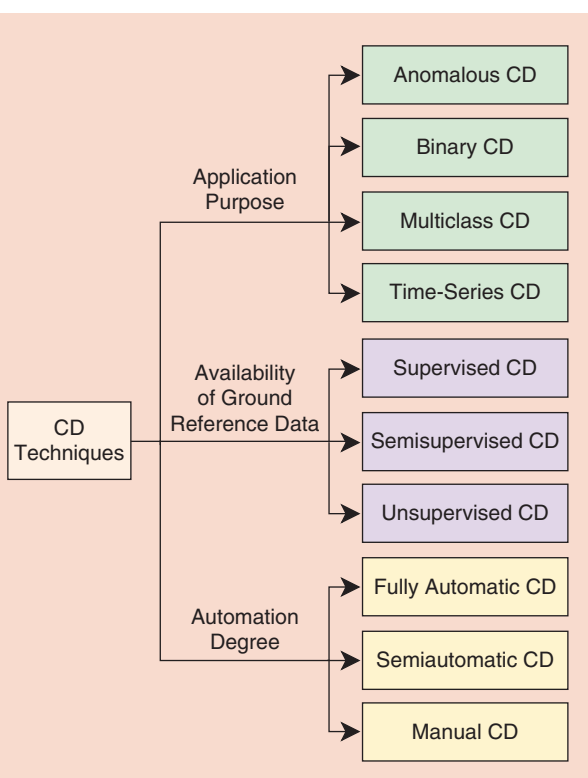


FIGURE 2. The categories of techniques for CD in HS images.

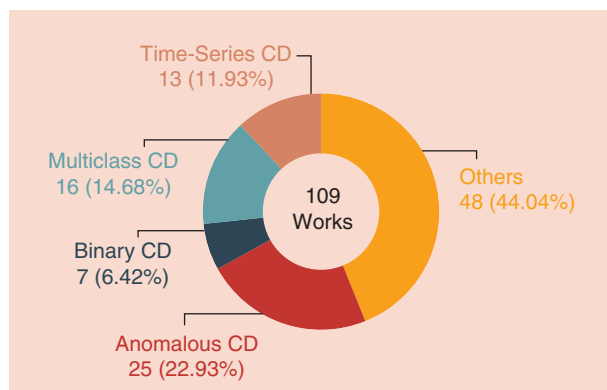


FIGURE 3. The statistics on CD as the subject of HS image articles published in IEEE journal and conference papers during the years 2012–2017, according to the category of CD application purpose.

scheme shown in Figure 4. The accurate preprocessing steps, such as uncalibrated and noisy band removal, bad band stripe repair, and radiometric and atmospheric corrections, among others, are usually necessary for enhancing the original spectral representation of the input HS images. In particular, an accurate coregistration process in HS images with a limited residual misregistration error significantly affects the performance of CD algorithms. Multitemporal analysis

acquired at times t_1 and t_2 , respectively. The corresponding pixels in two images represent the spectral signatures of the same area on the ground at the two dates. The difference image I_D can be obtained by comparing I_1 and I_2 with the vector differencing comparison operator, thus defining the CVA [16], [27], [30]–[32],

$$I_D = I_2 - I_1, \quad (1)$$

where each pixel in I_D corresponds to a B -dimensional spectral change vector (SCV).

Image stacking combines the multitemporal images by extending the data dimensionality toward the temporal direction. Let I_s be the stacked multitemporal images from two dates I_1 and I_2 :

$$I_s = [I_1, I_2], \quad (2)$$

where the dimensionality of I_s is $2B$. Then, proper techniques should be used in the full extended data dimensionality to extract the specific information associated with the changes.

Independent image analysis classifies each single time image using supervised classifiers and then compares the classification maps to discover changes. This is the most traditional CD method (also termed *postclassification comparison* [PCC]) [26] in both MS and HS images. It relies mainly on the availability of comprehensive ground reference data for generating the training samples as well as the selection of an effective classifier. However, collecting ground reference data is always an expensive and time-consuming process, and it becomes even more demanding when the ground references must be collected for multiple acquisition dates and for detailed land-cover classes. Therefore, the availability of multitemporal ground reference data is typically limited. Moreover, PCC suffers from the propagation of classification errors between two dates, which may significantly affect the CD accuracy. To deal with this issue, multitemporal classification techniques can be used (e.g., compound detection [33], [34]). However, these approaches require some multitemporal reference data. For these reasons, most articles in the literature address the CD problem by considering comparison operators (e.g., [28], [35]–[37]) and image-stacking operations (e.g., [38], [39]) (Figure 5).

Let $\Omega = \{\omega_n, \Omega_C\}$ be the set of all classes in the considered multitemporal images divided into the unchanged and changed classes, that is, ω_n and Ω_C , respectively. This definition represents the general case of ACD and binary CD, which aims to separate the changed targets (foreground) from the unchanged objects (background). For multiclass CD, the aim is not only to detect the general change class Ω_C but also to distinguish different classes. Therefore, Ω_C can be divided into K different kinds of change, that is, $\Omega_C = \{\omega_1, \omega_2, \dots, \omega_K\}$. This highlights how the CD problem can be divided into multiple subproblems, among which the most important ones are 1) discrimination between unchanged ω_n and changed samples Ω_C , 2) identification

IMAGE STACKING COMBINES THE MULTITEMPORAL IMAGES BY EXTENDING THE DATA DIMENSIONALITY TOWARD THE TEMPORAL DIRECTION.

tor, 2) an image-stacking approach, and 3) an independent image analysis. Afterward, specific CD techniques can be designed based on the change representation implemented in the previous step.

Described in greater detail, comparison operators model temporal variations in multitemporal images according to different techniques, such as univariate image differencing [26], change vector analysis (CVA) [27], index-based differencing [19], distance or similarity measures [16], and so on. A summary of the most widely used comparison operators can be found in [1]. To effectively use these comparison operators in HS images, it is crucial issue to select the most informative bands [28] or construct specific indexes based on the relevant bands (e.g., the HS vegetation indices [29]). Let I_1 and I_2 be a pair of B -dimensional HS images

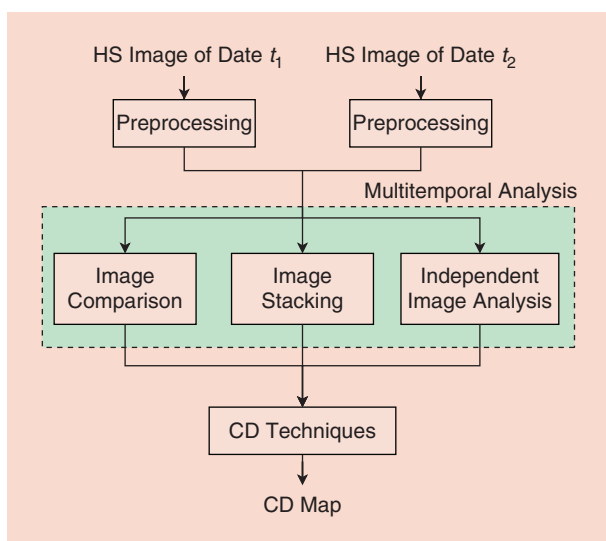


FIGURE 4. A block scheme of the CD approach in bitemporal HS images.

of the number of change types K , and 3) separation of the samples in Ω_C into the classes $\omega_k(k=1, 2, \dots, K)$ representing different kinds of change [11], [22].

In [35], the authors analyzed the concept of change in bitemporal HS images. A qualitative illustration example is shown in Figure 6. In particular, conceptually, SCVs can be separated into *major changes* and *subtle changes*. Major changes are related to land-cover transitions having spectral signatures that significantly differ from each other [Figure 6(a)]. Subtle changes show similar behavior to a given major change for most of the analyzed wavelengths but differ significantly in only some components of the spectrum [Figure 6(b)]. Subtle changes can be seen as subclasses of the corresponding major change. As an example, a major change representing a major land-cover transition (e.g., from noncultivated to cultivated) could be divided into subtle changes corresponding to different variations, such as water content or different growth rates of the crops. Although major changes may be discriminated by using MS images, this is not the case for subtle changes because they would be lost (i.e., grouped with the most similar major change) due to the coarse spectral resolution of such images.

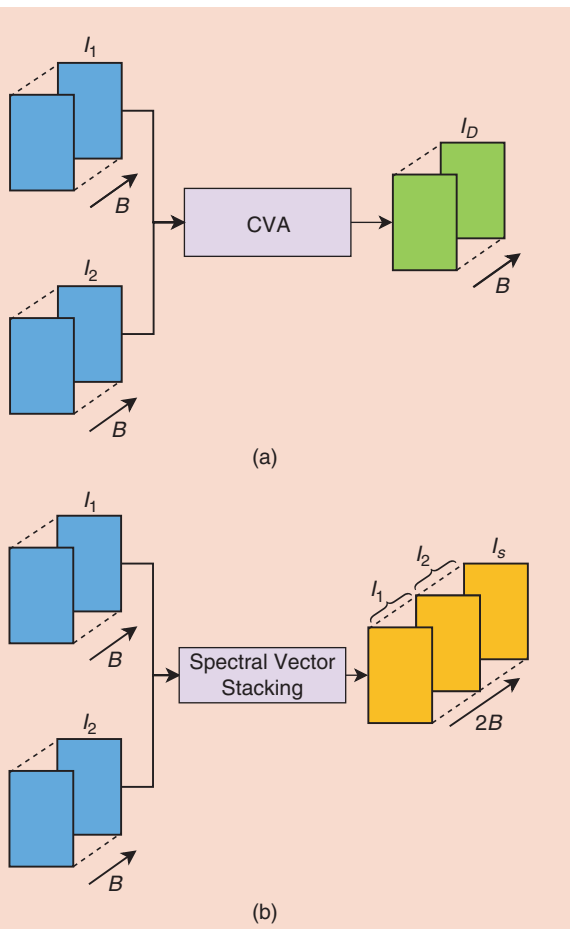


FIGURE 5. An illustration of the CD problem in HS images with (a) a comparison operator (i.e., CVA) and (b) an image-stacking operation.

Accordingly, HS images can be used to detect a wide variety of changes, ranging from major to subtle. A qualitative illustration of the major- and subtle-change concepts is shown in Figure 6. $\Omega_C = \{C_1, C_2, \dots\}$ is the set of major changes. Each major change may include subtle changes (i.e., $C_1 = \{C_{1,1}, C_{1,2}, \dots\}$ and $C_2 = \{C_{2,1}, C_{2,2}, \dots\}$). By iterating the process, it is possible to state that each subtle change can be further split until it is not possible to detect spectral inhomogeneity. Different changes can have significantly different relevance from a semantic point of view; depending on the application, one may be more interested in detecting the relevant but subtle land-cover transitions. The definition of what it is considered "change" is not straightforward and depends significantly on the application. Therefore, this aspect should be taken into account when developing CD methods for HS images—for example, by organizing the detected changes in such a way that the relevance of the different changes is highlighted [35].

DEPENDING ON THE APPLICATION, ONE MAY BE MORE INTERESTED IN DETECTING THE RELEVANT BUT SUBTLE LAND-COVER TRANSITIONS.

CHALLENGES OF CHANGE DETECTION IN HYPERSPECTRAL IMAGES

Although the use of HS images has key advantages in CD applications versus MS images, it also results in significant challenges that must be properly addressed to exploit the

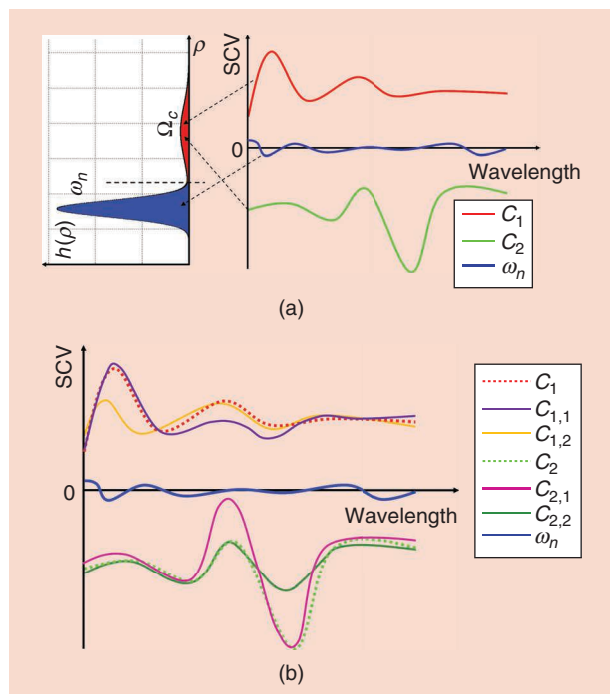


FIGURE 6. A qualitative illustration showing examples of (a) major changes and (b) subtle changes (solid line) within the given major changes (dotted line) defined in the SCV domain.

rich information content. These challenges are related to the automatic techniques required to extract the relevant change information.

One of the main challenges is related to the high dimensionality of HS data. The analysis of high-dimensional HS data spaces has proven to be complex and cannot be addressed with techniques developed for low-dimensional spaces [22], [28]. There are challenges in data handling, including storage volume and computing bottlenecks, that are actually common problems for all HS image processing tasks (i.e., classification, CD, target recognition). In the case of CD in HS images, such high dimensionality makes the extraction of changes from the feature space (e.g., differentiating features, stacking features) more challenging. Let us analyze the complexity of the problem.

An HS SCV is a spectral representation of how much the reflected radiance changed between two HS images acquired at different dates. Therefore, although on a single date each pixel carries the spectral signature describing the characteristics of the analyzed surface, in the multi-temporal case, we have a spectral signature for each pixel that describes the characteristics of the change (if present). Other comparison operators can also be considered [1]. Figure 7(a) and (b) shows two images acquired by the EO-1 Hyperion sensor over an irrigated agricultural area in Benton County, Washington, at two different times:

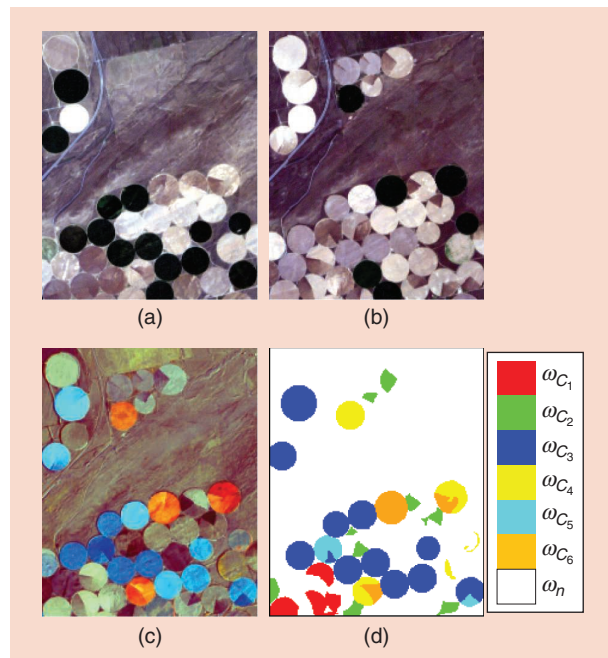


FIGURE 7. An example of a pair of bitemporal EO-1 Hyperion images and the resulting SCV image obtained by CVA. A false color composite (red: 650.67 nm; green: 548.92 nm; blue: 447.17 nm) was made of the original images acquired on an irrigated agricultural area in Benton County, Washington, in (a) 2004 (I_1) and (b) 2007 (I_2). (c) A composite of the three channels of the SCV image (I_D) (red: 823.65 nm; green: 721.90 nm; blue: 620.15 nm). (d) A change reference map. (Source: U.S. Geological Survey; used with permission.)

1 May 2004 (I_1) and 8 May 2007 (I_2). The major land-cover changes in this scenario are due to the transitions among crops, soil, water, and other land-cover types. Vegetation water content and crop-growth conditions may lead to the presence of the subtle changes. After the CVA is calculated, a false color composite of three channels of I_D is generated [Figure 7(c)], where different false colors indicate possible different kinds of change classes and gray areas represent the unchanged pixels. Figure 7(d) is the change reference map defined by a careful image interpretation, where six change classes are shown in different colors and the no-change class is in white. The Euclidean distance (ED)-based compressed change magnitude ρ of the SCV image I_D can be calculated to discriminate between changed and unchanged areas [31]:

$$\rho = \sqrt{\sum_{b=1}^B (I_D^b)^2}. \quad (3)$$

Unchanged pixels show values close to 0, whereas changed pixels show larger-magnitude values. The histogram of the magnitude image of the Benton County data set is shown in Figure 8. A threshold (red line in Figure 8) can be defined through either manual selection [40] or automatic estimation based on a certain mixture of distributions (e.g., Gaussian) [41]. In HS images, the separation of change and no-change classes with the change magnitude is more complex in terms of the MS case, leading to an increase of omission and commission errors. This is because there might be subtle changes affecting only a limited number of bands, thus exhibiting a small magnitude. Moreover, discrimination of the multiple change classes within Ω_C also becomes more challenging in the HS case.

Another significant problem of HS images is data redundancy. Because a typical HS sensor performs a nearly continuous measurement of the spectrum, for a given pixel, adjacent spectral channels have a high probability of containing very similar values of reflected radiance. Therefore, increasing the spectral resolution does not increase

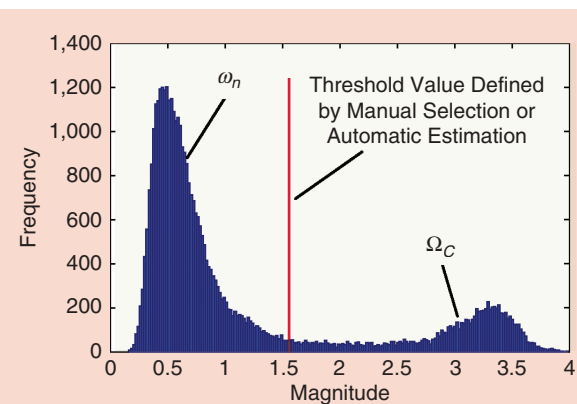


FIGURE 8. A histogram of the change magnitude image based on the Benton County Hyperion data set.

the information content indefinitely. Figure 9 shows the R^2 correlation matrix computed on the I_D image of the Benton County Hyperion data set. R^2 represents the correlation of each SCV band with the other ones. Four main correlated band groups can be observed, and the adjacent bands are highly similar. This indicates the redundancy present in the considered HS data set. When we look for changes in the multitemporal domain, we expect more redundancy in the HS change vectors than in the spectral vectors of each single image.

Noise generated by both external sources (atmospheric effects due to absorption and scattering) and internal sources (instrument noise) also affects HS sensors. These noise sources are also present in MS sensors. The atmospheric haze can be mitigated with atmospheric correction techniques, such as atmospheric removal (i.e., ATREM) [42] or fast line-of-sight atmospheric analysis of spectral hypercubes (i.e., FLAASH) [43] algorithms. Instrument noise is introduced by 1) nonideal electronics (thermal and shot noise); 2) quantization; 3) malfunctioning sensors, which generate impulsive noise or missing pixels/lines; and 4) striping noise due to a calibration error of the array of sensors in push-broom scanners [11]. When the spectral resolution increases, the measured reflectance at the sensor decreases, whereas the signal-independent noise, such as the thermal noise, does not, thus decreasing the signal-to-noise ratio [44]. When the number of bands increases above a certain limit, information represented by the HS bands becomes more sparse and implicit, which may degrade the discriminative ability of a CD, especially in identifying multiclass changes.

CHANGE DETECTION TECHNIQUE IN MULTITEMPORAL HYPERSPECTRAL IMAGES

Table 2 shows a nonexhaustive summary of existing CD methods in HS images according to the categorization related to the CD application presented in the “Categories of Change-Detection Approaches for Hyperspectral Images”

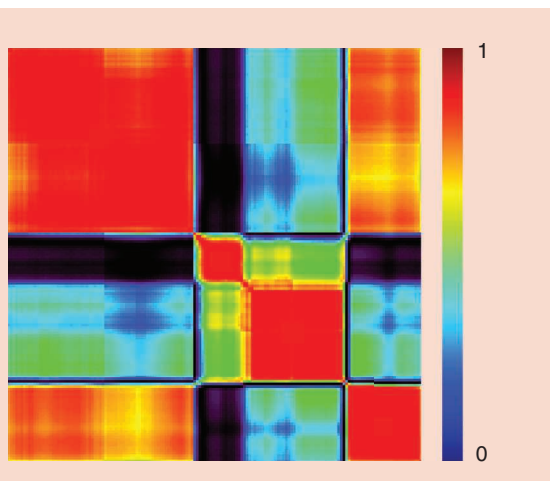


FIGURE 9. The R^2 correlation matrix of the I_D image, where four highly correlated adjacent band groups indicate the redundancy.

section. In this section, we provide an overview of the main techniques proposed in the literature for the different categories.

ANOMALOUS CHANGE DETECTION

ACD aims at identifying anomalous changes between images by suppressing background and accentuating changes [76]. In general, ACD approaches for HS images can be separated into single-instance and multi-instance target detection [56]. The key point is to investigate the statistics of the images, increase the detection probability of changes caused by human activity, and suppress background in the image scene sequences. For ACD, special attention is usually paid to the detection of small changes resulting from the insertion, deletion, or movement of manufactured small objects as well as from small

TABLE 2. SUMMARY OF MAIN TECHNIQUES FOR CD IN HS DATA (THE TABLE IS NOT EXHAUSTIVE).

APPLICATION	TECHNIQUE	REFERENCE
ACD	Chronochrome	Schaum and Stocker [45]
	Covariance equalization	Schaum and Stocker [46]
	Clustering	Shimoni et al. [47]
	Statistical modeling	Theiler et al. [48]
	Reed-Xiaoli algorithm	Acito et al. [49]
	Model based	Wu et al. [50]
	Error and noise mitigation	Zhou et al. [51]
		Meola et al. [52]
		Theiler and Wohlberg [53]
		Vongsy et al. [54]
Binary CD	Transformation	Meola et al. [55]
		Meola and Eismann [56]
		Eismann et al. [57]
		Frank and Carty [58]
		Nielsen [59], [60]
		Ortiz-Rivera et al. [61]
		Hemissi et al. [62]
		Liu et al. [63]
		Wu et al. [64]
	Unmixing	Du et al. [65]
Multiclass CD		Ertürk and Plaza [39]
		Ertürk and Plaza [66]
		Ertürk et al. [67]
	Others	Yuan et al. [68]
		Du et al. [69]
Time-series CD	Clustering	Chen and Wang [70]
	Compressed CVA	Liu et al. [35]
	Band selection	Liu et al. [36], [37]
	Unmixing	Liu et al. [28]
	Binary SCVs	Liu et al. [38]
Time-series CD	Clustering	Marinelli et al. [71]
	Unmixing	Yang and Sun [72]
		Hemissi et al. [73]
		Henrot et al. [74]
		Veganzones et al. [75]

stationary objects that have spectrum changes between images, such as in the case of camouflage, concealment, and deception [49].

In the literature, approaches such as chronochrome [45] and covariance equalization [46] are classical algorithms for ACD. They investigate a linear prediction of posttime data using the statistics of both pretime and posttime data sets to discover and highlight the anomalous changed pixels against the unchanged background. In greater detail, in [45], the authors compute the covariance matrices of the spectral signatures at times t_1 and t_2 and the cross-temporal covariance matrix. Then, they compute the chronochrome prediction error between the real signatures at t_2 and the ones predicted using the chronochrome. The prediction error is then

used in the Reed-Xiaoli (RX) anomaly detector to identify changes. In [46], the authors consider a covariance-equalization implementation that is meant to be more robust to registration errors. They exploit an ACD approach based on the assumption that the

mean spectral signature of the target is known. They also use a combination of chronochrome and matched filtering. In [47], three iterative clustering methods, that is, class-conditional covariance equalization (QCE), bitemporal QCE, and wavelength-dependent segmentation, were applied to detect human-caused changes in VNIR and thermal-IR HS images. The results prove that the use of a spatially adaptive detector greatly enhanced ACD performance in the target CD in terms of false alarm reduction.

Some techniques focused on modeling data variables from different perspectives have recently been proposed. For instance, in [48], the anomalous changes in HS images were modeled and detected according to elliptically contoured distributions. This is motivated by the fact that, because the problem is the detection of anomalous changes (which are rare), there is a high probability that these changes are represented in the tail of the statistical distribution. Therefore, elliptically contoured distributions may be more suitably compared with Gaussian distribution. In [50], the change residual image is computed based on slow feature analysis (SFA), and changes are detected with the RX anomaly detector. SFA is used to compute the change residual image in which the unchanged areas and large areas affected by changes show small values. This makes the problem of ACD a classical anomaly-detection problem, which is solved using the RX algorithm.

In [51], a cluster kernel RX algorithm is presented that clusters the background samples while using the cluster centers for anomaly detection. The clustering step is used to cluster the background pixels, which are then replaced with the corresponding cluster centers. The RX is subsequently applied to the new samples, reducing the computation load. An improved ACD approach that exploits a model-based

method is proposed in [52]. It is extended for use on both relatively calibrated and uncalibrated HS images and applied to airborne HS images. In [64], the authors propose a subspace-based CD method using undesired class information as prior knowledge. A subspace distance was computed to determine that the anomalous pixels have changed when compared with the background subspace.

Recently, a tutorial on the ACD problem in HS images within a theoretical Gaussian framework was presented [49]. This tutorial addresses several solutions based on the statistical detection theory by formulating the ACD as a binary decision problem. Using the multivariate Gaussian model, it presents a rigorous statistical framework to explain the detectors by changing 1) the decision rule (hyperbolic or elliptical), 2) the observation vector model, and 3) the local or global Gaussian model. Some other useful theoretical information is provided, including the presentation of a freely available validation data set. A comprehensive experimental comparison is also carried out to show the performance of different ACD algorithms. In the literature, there are also some other works focused mainly on the detection of specific changes by addressing specific issues, for example, eliminating image parallax errors [54], registration errors [53], [56], vegetation and illumination changes [55], and diurnal and seasonal variations [57].

BINARY CHANGE DETECTION

Binary CD is one of the typical and popular CD applications of recent decades. Its objective is to detect and separate the change and no-change classes in the considered multitemporal images. Accordingly, from the spectral point of view, pixels with significant spectral variations between the considered dates have higher probability to be changed and vice versa. A common way to identify binary information based on comparison operators, such as CVA, is to construct the compressed change magnitude information ρ as in (3). Other methods focus on the construction of binary representations based on similarity measures, such as the spectral angle mapper (SAM) [77] or spectral information divergence [78]. Therefore, it is possible to use approaches similar to those developed for binary CD in MS because the full dimensionality of data is compressed into one magnitude feature space. However, the information redundancy in the adjacent bands might affect the change magnitude and, thus, the binary CD performance, so the selection of the most informative band subsets is crucial, as pointed out in [28]. Based on the magnitude image, it is possible to model the specific statistical distribution of the two classes (e.g., by Gaussian mixture [41] or Rayleigh-Rice mixture [79]) under the Bayesian framework and then use thresholding techniques to generate the CD map. In [41] and [79], the statistical distribution parameters are estimated using the expectation maximization (EM) algorithm.

Another major group of classical binary CD methods in HS images is designed based on the features extracted by using data transformation techniques. The original

**ANOTHER SIGNIFICANT
PROBLEM OF HS IMAGES IS
DATA REDUNDANCY.**

high-dimensional HS data are transformed into a few components where change information can be compressed and highlighted. In this context, multivariate alteration detection (MAD) based on canonical correlation analysis was proposed in [80] and applied to monitor vegetation changes in HS images [58]. The aim of MAD is to find a linear transformation of the two HS images such that a measure of change is maximized. In particular, the linear transformation aims at maximizing the variance of the difference of the two transformed multitemporal data. The extended version, termed *iterative reweighted MAD* (IR-MAD), was proposed in [59] to better model the change and no-change background representations. IR-MAD is an iterative version of MAD based on the reweighting of the individual samples. In particular, at each iteration, each pixel is weighted according to a measure based on the sum of the squared MAD variables (chi-squared distributed).

Temporal principal component analysis (PCA), which was proposed in [61], exploits the variances in PCs after transforming the differencing and stacking multitemporal images, respectively. Thus, the no-change and change classes are associated with specific PCs. In [60], two kernel versions of maximum autocorrelation factor (MAF) analysis and minimum noise fraction (MNF) analysis were introduced for CD. The experimental results showed that the kernel MAF/MNF performed better than its linear version and the kernel PCA. Such transformation-based methods require a strong interaction with the end users to select the most informative multitemporal components to emphasize specific changes. This step is usually time consuming, especially when the number of changes in HS images is large. Although transformation-based approaches can enhance the change information and reduce redundancy in the HS bands, they are not able to automatically identify the real number of multiclass changes, which may limit the use of these methods in practical applications.

Several recent articles have presented solutions to the binary CD problem in HS images. In [62], a spatiotemporal independent component analysis (stICA) is designed for extracting the spatiotemporal patterns from different HS sensors or from different acquisition conditions and dates. The aim of the stICA is to reach signal data independence both in the spatial and temporal domains. In [63], ICA is applied with the uniform feature design strategy in a hierarchical framework, focusing on the detection of the specific crop-land vegetation changes. In [68], a semisupervised method is developed under a Laplacian regularized metric framework, where a distance metric is learned for detecting changes under noisy conditions. In [69], a simple but effective relative radiometric normalization method is developed, and two automatic binary CD approaches after normalization are introduced, including a kurtosis-maximization-based analysis and a distinct change-vector extraction and classification. In [70], the authors propose a spectrally–spatially regularized low-rank and sparse decomposition model for

binary CD. The proposed method decomposes the SCV image into three different components: 1) a locally smoothed, low-rank matrix for the clean change features; 2) a sparse matrix for the outliers; and 3) an error matrix for the small Gaussian noise. The final change map is obtained based on k-means clustering applied to the extracted change features.

There are also recent articles that address the considered binary CD problem in HS images from the subpixel point of view. In [65], a linear mixture model is applied to analyze the endmembers and abundances estimated from each single-time HS image to address the binary CD problem. In [39], the potential of unmixing for binary CD is investigated based on stacked multitemporal HS images. In [66] and [67], sparse unmixing methods are exploited, and the results show the advantages of these methods in enhancing binary CD performance. Although unmixing CD methods can also provide results in terms of abundances of endmember spectra, these articles provide results only in terms of binary CD.

We carried out an analysis to compare some binary CD techniques using the Benton County Hyperion data set. For generating the binary change index images, we considered the ED magnitude (ED-Mag) [31], IR-MAD magnitude (IRMAD-Mag) [59], and SAM similarity image (SAM-SI) [77]. Then, we used four binary CD techniques, including Otsu segmentation [81], EM algorithm based on the Gaussian mixture (EM-GM) [41], EM algorithm based on the Rayleigh-Rice mixture (EM-RRM) [79], and fuzzy c -means (FCM) [28], to generate the binary change maps. The qualitative comparisons of the three change index images and the binary change maps are provided in Figures 10 and 11, respectively. The quantitative experimental results are provided in Table 3. We can see that, in this case, the ED-Mag image better represents the binary change information (including both the major and subtle changes) that occurred in the scene, whereas the IRMAD-Mag and SAM-SI images suppress more background information but also eliminate some subtle changes. Among the four binary CD

MULTICLASS CD PLAYS A VERY IMPORTANT ROLE IN HS IMAGES.

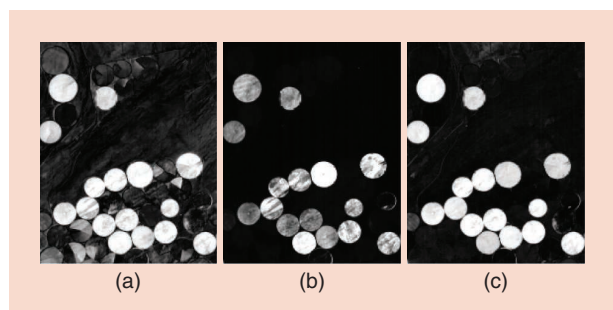


FIGURE 10. Three binary change index images obtained on the Benton County data set: (a) ED-Mag, (b) IRMAD-Mag, and (c) SAM-SI.

algorithms, the EM-GM approach performed better than the other three methods when considering the ED-Mag image, whereas EM-RRM and FCM achieved better results on the IRMAD-Mag and SAM-SI images, respectively. In general, the selections of both a suitable binary change index image and a robust binary CD approach are key factors for a successful CD application.

MULTICLASS CHANGE DETECTION

Multiclass CD plays a very important role in HS images. Its goal is to detect and identify different kinds of changes associated with different land-cover transitions, material composition changes, or other dynamic variables, such as moisture conditions. Compared with ACD and binary CD tasks, the multiclass CD task is more complex and,

thus, challenging because its aim is not only to detect the changes but also to discriminate different change classes. If comprehensive multitemporal ground reference data are available, multiclass CD can be carried out using PCC [26] (considering the independent classification on each single date image) or direct multideate classification [82], [83], relying on stacked multitemporal HS images. The main advantage of these supervised approaches is that they can provide detailed “from-to” land-cover transition information. However, it is often very difficult (or even impossible) to have comprehensive multitemporal ground reference data. Therefore, designing advanced unsupervised or semisupervised CD techniques to be as independent as possible from the ground reference data is one of the most important tasks for multiclass CD in HS images.

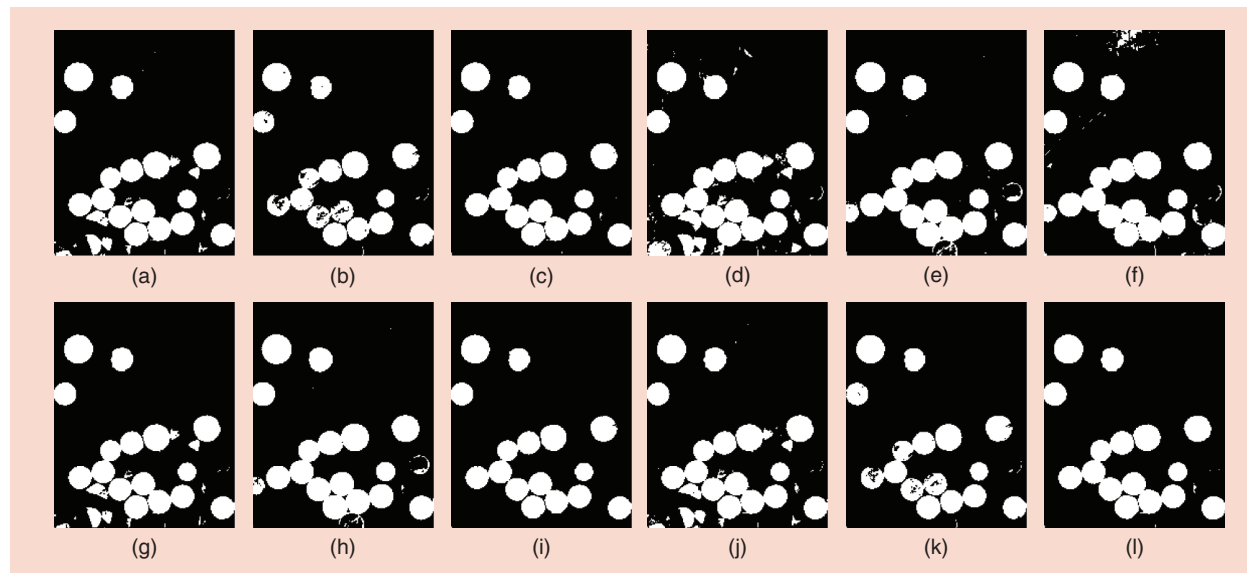


FIGURE 11. Binary change maps obtained on different change index images by different algorithms: (a), (d), (g), and (j) ED-Mag; (b), (e), (h), and (k) IRMAD-Mag, and (c), (f), (i), and (l) SAM-SI. (a)–(c) The Otsu segmentation. (d)–(f) The EM-GM thresholding. (g)–(i) The EM-RRM thresholding. (j)–(l) The FCM clustering.

TABLE 3. QUANTITATIVE BINARY CD RESULTS OBTAINED BY SOME OF THE CONSIDERED TECHNIQUES ON THE BENTON COUNTY HYPERION DATA.

CHANGE, INDEX IMAGES	METHODS	OA, %	K	OE, PIXELS	CE, PIXELS	TE, PIXELS
ED-Mag	Otsu	95.25	0.8629	1,896	28	1,924
	EM-GM	96.55	0.9034	1,195	203	1,398
	EM-RRM	94.91	0.8521	2,048	15	2,063
	FCM	95.46	0.8694	1,800	40	1,840
IRMAD-Mag	Otsu	91.65	0.7453	3,368	12	3,380
	EM-GM	93.02	0.7991	2,300	528	2,828
	EM-RRM	93.19	0.8028	2,357	400	2,757
	FCM	92.11	0.7608	3,184	12	3,196
SAM-SI	Otsu	93.20	0.7976	2,726	27	2,753
	EM-GM	92.55	0.7871	2,293	726	3,019
	EM-RRM	92.71	0.7811	2,945	6	2,951
	FCM	93.31	0.8014	2,672	36	2,708

CE: commission errors; K: kappa coefficient; OA: overall accuracy; OE: omission errors; TE: total errors.

As pointed out in the “Change-Detection Problem in Hyperspectral Images” section, three subproblems should be properly addressed in multiclass CD in HS images: the binary CD, identification of the number of changes, and multiclass change discrimination. Each subproblem deserves to be analyzed in detail, with proper techniques designed to generate a reliable output. In the literature, some recent works have addressed this issue.

In [35], taking into account the intrinsic complexity and structure of CD in HS images, the authors provide a definition of the change concept in HS images from the SCV perspective, where major and subtle changes are properly defined with respect to the spectral change significance. A hierarchical spectral change analysis is conducted by investigating, in detail, the spectral variations from coarse to fine processing levels, leading to a better modeling of the complex change structure. An unsupervised hierarchical spectral CVA (HSCVA) method is proposed for analyzing the change clusters at different levels of spectral variations. At each level, an initialization is implemented to drive an automatic change model selection to discover the number of multiple changes, and then a clustering procedure is applied to identify the multiclass change information.

In [36], the authors propose a semisupervised sequential spectral CVA (S^2 CVA) technique for discovering and discriminating multiclass changes in HS images. Based on the original version of the compressed CVA (C^2 VA) technique [27] (which was proposed for CD in MS images), the S^2 CVA iteratively analyzes the heterogeneous change information by following a top-down structure. Therefore, the complex change information in the original high-dimensional feature space is adaptively and iteratively compressed and projected into a sequence of 2D feature spaces. Each of them is associated with a specific portion of the whole SCV space. At each level of detection (here, taking the first level as an example), change patterns are represented in a 2D polar domain that is constructed by the change magnitude ρ in (3) and the change direction θ [36], where

$$\theta = \arccos \left[\left(\sum_{b=1}^B (I_D^b r^b) \right) / \sqrt{\sum_{b=1}^B (I_D^b)^2 \sum_{b=1}^B (r^b)^2} \right]. \quad (4)$$

The reference vector r is defined as the first eigenvector that corresponds to the largest eigenvalue after eigen-decomposition

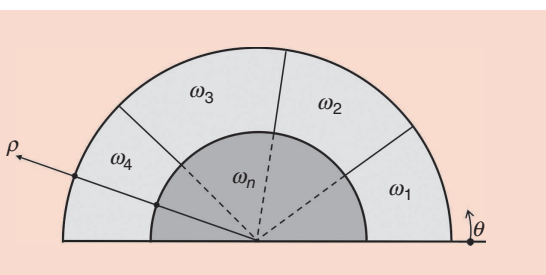


FIGURE 12. A 2D compressed polar domain for representing multiclass information [27], [28], [36].

of the covariance matrix of I_D . The adaptive reference vector results in an improved change representation by projecting the considered SCV samples into a direction that maximizes the variance of the measurement while preserving the discriminative information of changes [36]. Change and no-change pixels can be separated along the change magnitude axis, whereas the homogeneous change clusters associated with the number of multiclass changes can be identified along the direction axis (Figure 12). A sequential analysis can be driven by focusing on each specific identified change cluster, which allows a further subtle change identification.

Examples of the change magnitude and direction images are shown in Figure 13(a) and (b), respectively. Based on two change variables, the 2D compressed change representation at the first-level detection using the S^2 CVA approach is illustrated in Figure 14, where four major changes (i.e., from C_1 to C_4) can be identified. Each can be further analyzed at the next levels of sequential detection until no

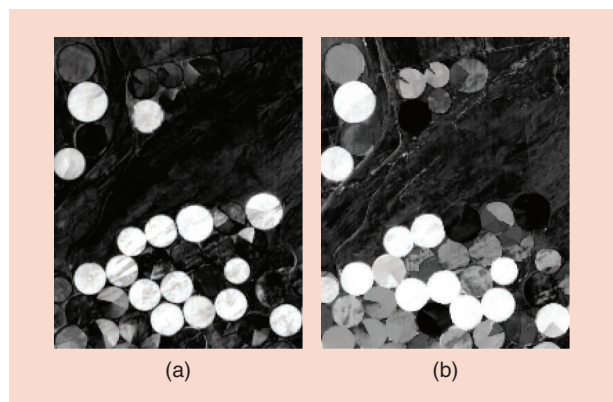


FIGURE 13. The change variables computed based on sequential spectral CVA at its first level of detection (Benton County Hyperion data set). (a) The change magnitude image. (b) The change direction image.

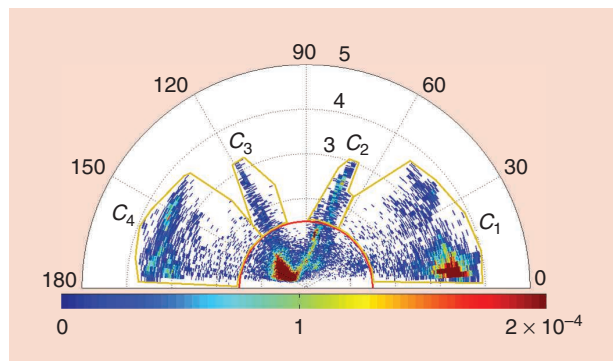


FIGURE 14. A 2D change representation scattergram obtained at the first level of the S^2 CVA hierarchy (Benton County Hyperion data set). A binary CD decision threshold value is defined using EM-GM thresholding (red semicircle) and discrimination boundaries between different change types (shown as yellow polygons). Four major changes can be identified and will be further analyzed at the next iteration after sequential processing in S^2 CVA.

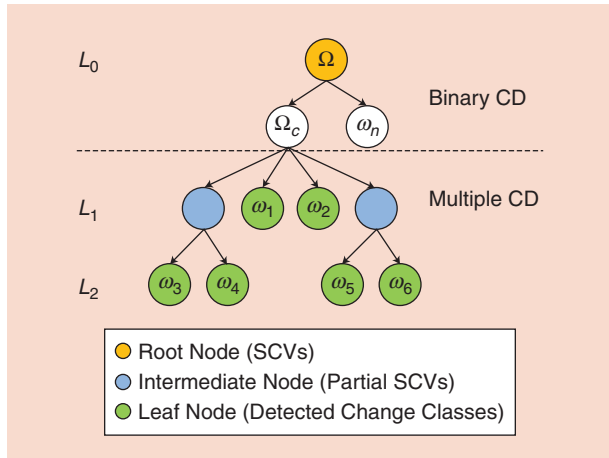


FIGURE 15. A three-level hierarchical tree for modeling the multiclass CD problem (Benton County Hyperion data set) with S²CVA.

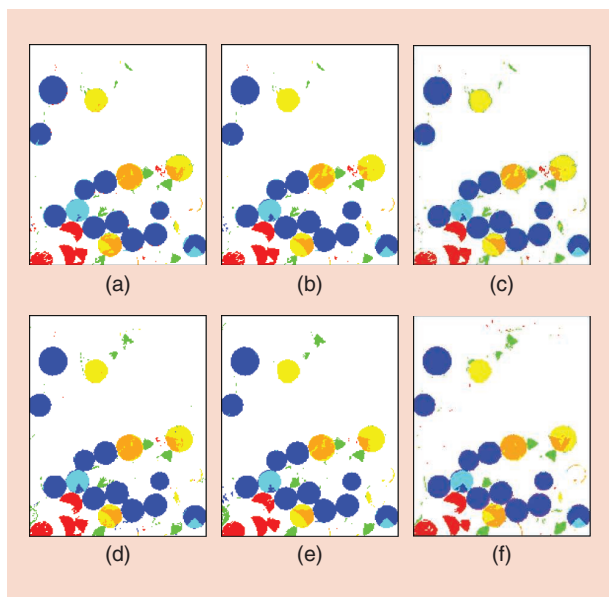


FIGURE 16. Multiclass change maps obtained on the Benton County Hyperion data set using (a) HSCVA [35], (b) S²CVA [36], (c) BSCVs [71], (d) band selection and support vector machine [28], (e) S²MCD [37], and (f) multitemporal spectral unmixing [38] approaches. The detected change classes are represented in different colors, and the no-change classes in white.

heterogeneous change classes are present in the 2D feature space. In the example, six changes (i.e., $\omega_1-\omega_6$) were detected by following the three-level (i.e., L_0-L_2) tree hierarchy shown in Figure 15, where the leaf nodes correspond to the six change classes. The multiclass change map is shown in Figure 16(b).

In [71], the authors propose an unsupervised multiclass CD method based on binary SCVs (BSCVs), which converts the original SCVs into binary code words that highlight the change information. The binarization of the SCVs moves to a simpler domain that can be exploited to discriminate the different kinds of change. The BSCVs are then represented into a dendrogram (i.e., a tree structure) to separate the types of change, taking into account the hierarchical organization of the change components. The binary representation is effectively exploited to construct the dendrogram because it represents the change information in a simpler and more explicit way compared with the real value representation (i.e., the SCVs).

In [28], the authors analyze in detail the CD performance on HS images by selecting the most informative band subset from the original high-dimensional HS data space. Several issues are investigated, including 1) the estimated number of multiclass changes, (2) binary CD performance, (3) multiple CD performance, (4) estimated optimal number of selected bands, and (5) computational efficiency. In particular, both supervised and unsupervised CD approaches are studied. Experimental results obtained on different data sets demonstrate that it is feasible to perform the considered CD task for HS images in a reduced feature space without losing the discrimination capabilities of a change detector.

In [37], a semisupervised technique [termed *semisupervised multiclass change detection (S²MCD)*] is proposed to enhance the multiclass CD performance in HS images. It takes advantage of the unsupervised change representation, i.e., the compressed adaptive SCV representation in the 2D polar domain [36], to provide prior knowledge of the multiclass change information. Then, the pseudotraining samples are generated for the no-change class and for each change class based on a stratified random-sampling strategy. The multiclass CD task is completed with high detection accuracy using the generated pseudotraining samples and advanced supervised classifiers, such as SVM and random forest for classifying the original SCV or transformed features.

The results of a qualitative and quantitative experimental comparison of some state-of-the-art multiclass CD methods applied to the Benton data set are provided in Figure 16 and Table 4. We considered the following methods in the experiments: HSCVA [35]; S²CVA [36]; BSCVs [71]; BS-SVM, where the 18 most informative bands were selected [28]; S²MCD (using the RF classifier on the first 10 MNF components) [37]; and MSU [38]. The first three approaches are unsupervised, which is useful in practical applications when the ground reference data are not available. The last

TABLE 4. MULTICLASS CD RESULTS OBTAINED WITH STATE-OF-THE-ART TECHNIQUES ON THE BENTON COUNTY HYPERION DATA.

METHODS	OA, %	K	OE, PIXELS	CE, PIXELS	TE, PIXELS
HSCVA [35]	95.26	0.8800	1,715	1,918	3,633
S ² CVA [36]	95.36	0.8822	1,878	1,676	3,554
BSCVs [71]	94.72	0.8662	1,935	2,138	4,073
BS-SVM [28]	96.37	0.9089	1,245	1,469	2,714
S ² MCD [37]	96.25	0.9055	1,323	1,519	2,998

two approaches are supervised. Taking advantage of the selected bands (i.e., BS-SVM) or transformed features (i.e., S²MCD) and the robust classifiers, they result in better CD performance in terms of higher accuracies.

These works mainly focus on the detection of multiclass changes at the pixel level. In the literature, there are few works addressing CD at the subpixel level. In [84], CD is implemented at the subpixel level based on nonlinear spectral unmixing and decision fusion, where the inner-pixel subtle changes are analyzed and multiple land-cover compositions are combined. Although it was originally designed for CD in MS images, this technique can also be applied to HS images with the available reference training data. An unsupervised MSU model is proposed in [38]. It investigates the spectral-temporal mixture properties in multitemporal HS images, and the CD problem is solved by analyzing the abundances of different distinct multitemporal endmembers (including both change and no-change classes) at the subpixel level (an example of extracted multitemporal endmembers in the MSU approach on the Benton County

Hyperion data set is shown in Figure 17). By taking advantage of the endmembers extraction and change and no-change spectral compositions within a pixel, the identification of the number of changes is performed by identifying the distinct endmembers, and the discrimination of multiclass changes is addressed by linear unmixing and abundance analysis. Reliable CD outputs are obtained, and subpixel-level spectral variations not detected with the pixel-level CD techniques are identified. An example of subpixel-level multiclass CD results on the Benton County data set is shown in Figure 18. The MSU approach identified seven change classes, whereas the aforementioned pixel-level methods identified six classes. The new change (i.e., class 7) is associated with the change of roads surrounding irrigated agricultural fields. Because the road width is less than a full

**IN THE LITERATURE,
THERE ARE FEW WORKS
ADDRESSING CD AT
THE SUBPIXEL LEVEL.**

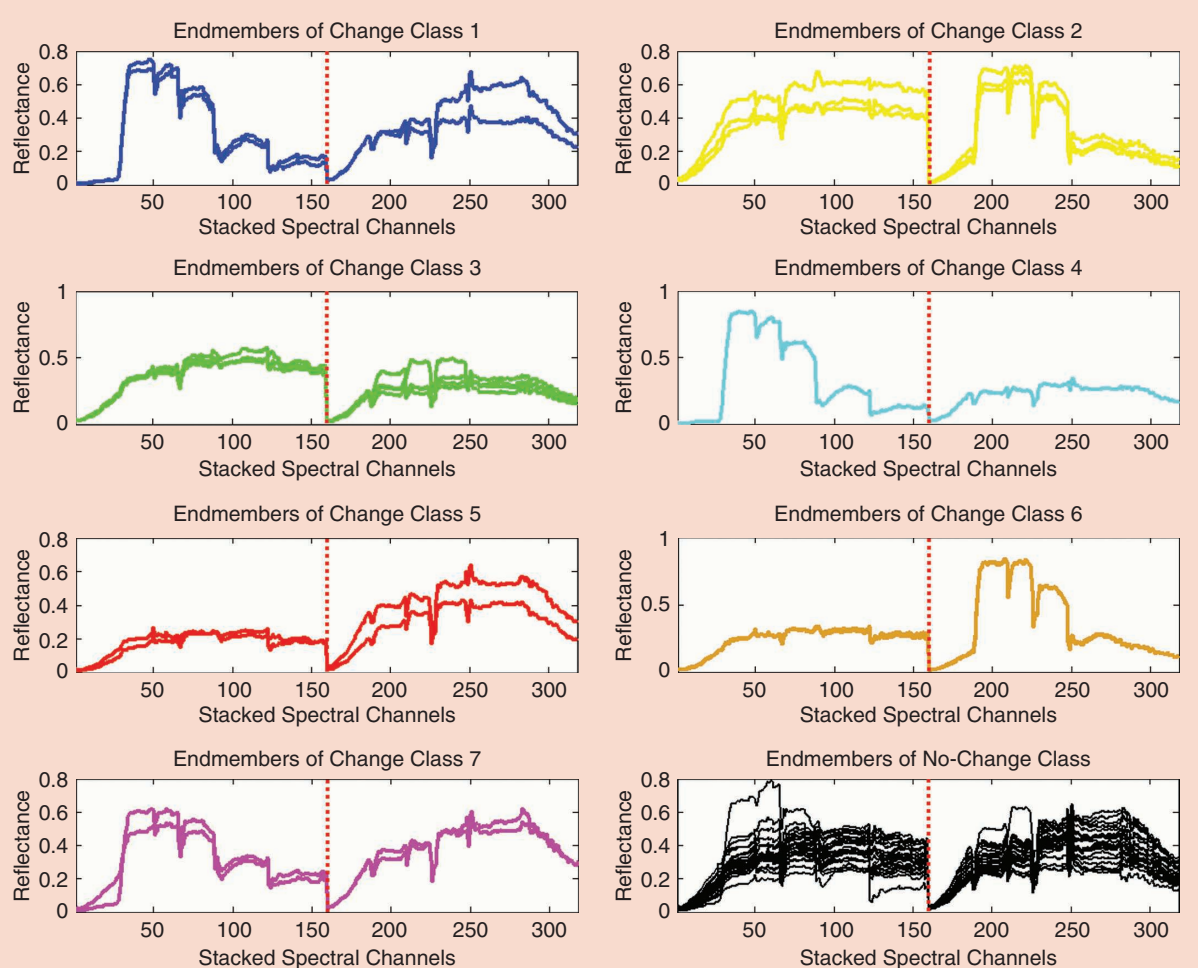


FIGURE 17. The endmembers extracted by the MSU approach on the Benton County Hyperion data set. Seven unique change classes are identified and shown in different colors; the no-change endmembers are in black. The endmembers present some variability within the same class.

pixel (which represents 30 m), it results in a spectral change at the subpixel level.

CHANGE DETECTION IN IMAGE TIME SERIES

CD in the time series of HS images requires the availability of a long time sequence of HS images. The user-interest

changes may be either abrupt changes that occurred on the land surface or subtle changes in a given time period. The latter are valuable to reveal land-cover evolution trends by investigating change patterns from the time perspective. From current HS satellites, it is still difficult to have a high temporal resolution (e.g., EO-1 Hyperion had a revisit time between 16 and 30 days). Thus, it is difficult to construct long time series for change analysis. For future HS satellite missions (see Table 1), which will have a decreasing revisit-time resolution, the use of a denser time series of HS images will provide opportunities to detect subtle changes in the land surface. Until now, in the context of HS image time series CD, there are few works in the literature due to the limitations of not having a long time series of HS images in real applications.

In [72], an unsupervised CD method is proposed for detecting small changes in a multitemporal HS image sequence. The feature space was built using block processing and locally linear embedding, whereas the CD map was generated by clustering the change and no-change binary classes.

A framework for dynamically modeling and efficiently unmixing a time series of HS images is proposed in [74]. Based on the linear mixing process at each time, the spectral signatures and fractional abundances of the pure materials in the scene are viewed as latent variables that follow a dynamic structure. An efficient spectral unmixing algorithm is developed to estimate the latent variables by performing alternating minimizations.

In [75], the authors apply canonical polyadic tensor decomposition techniques to the blind analysis on HS big data that can be either time series or multiangular acquisitions. The method can be interpreted as multi-linear blind spectral unmixing, where the big HS tensor is decomposed into three factors, such as spectral signatures, fractional spatial abundances, and temporal/angular changes. Both quantitative and qualitative evidence of the validity of this methodology were obtained using the MODIS HS data set during the 2012 snow season in the French Alps.

CONCLUSIONS

The role of multitemporal HS images is becoming increasingly important in remote sensing applications. They provide finer and deeper insights to discover, describe, and discriminate the land-cover changes on Earth's surface. Multitemporal HS images are an important data source for CD applications to detect both abrupt and subtle changes using bitemporal images and long time series. With the numerous HS missions that will be launched in the near future, the number of multitemporal HS data sets will significantly increase. This will require the design of advanced techniques to take full advantage of HS images in the multitemporal framework.

In this article, the problem of CD in HS images was analyzed in terms of basic concept definition, category description, and discussion

WITH THE NUMEROUS HS MISSIONS THAT WILL BE LAUNCHED IN THE NEAR FUTURE, THE NUMBER OF MULTITEMPORAL HS DATA SETS WILL SIGNIFICANTLY INCREASE.

and 30 days). Thus, it is difficult to construct long time series for change analysis. For future HS satellite missions (see Table 1), which will have a decreasing revisit-time resolution, the use of a denser time series of HS images will provide opportunities to detect subtle changes in the land surface. Until now, in the context of HS image time series CD, there are few works in the literature due to the limitations of not having a long time series of HS images in real applications.

In [73], the authors propose a method for modeling the temporal variation of the reflectance response as a function of time period and wavelength. It is designed based on a

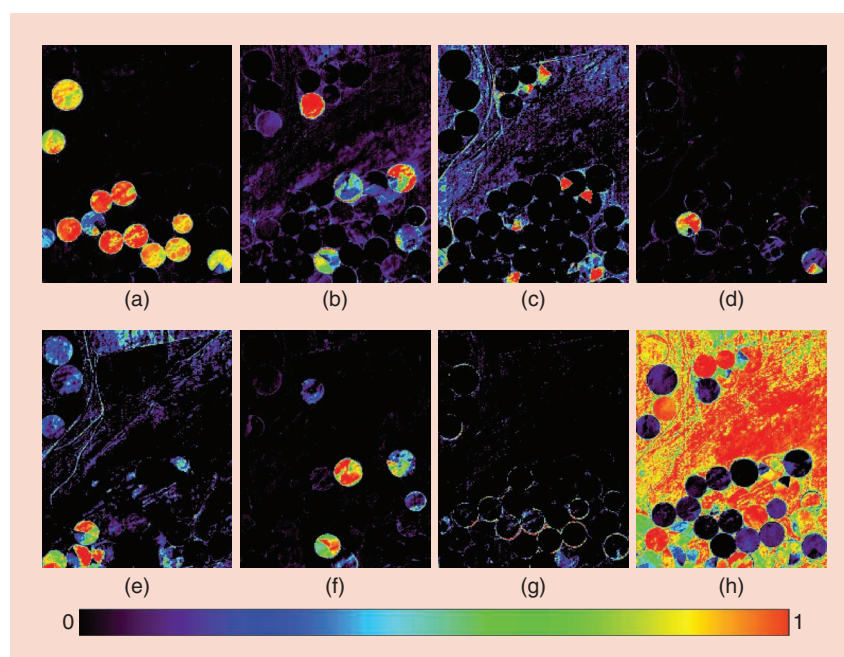


FIGURE 18. The subpixel-level multiclass CD results, i.e., class abundances, obtained using the MSU approach on the Benton County Hyperion data set [38]. (a)–(g) The seven change classes. (h) The no-change class.

of challenges. We provided an overview of the main CD methods for HS images available in the literature, including the most popular standard techniques and recently proposed ones. Four CD applications in HS images were considered: 1) ACD, 2) binary CD, 3) multiclass CD, and 4) time series CD. Each application was analyzed in detail, from basic concepts to a literature overview of recent developments. We also provided a comprehensive review focused on recent published works related to CD in HS images. Qualitative and quantitative examples of experimental results were illustrated by comparing the accuracies of some state-of-the-art binary and multiclass CD approaches on a real Hyperion data set.

In general, there are still many open issues that require further analysis, such as implementing an accurate preprocessing of multitemporal HS images, generating highly representative change features from the high-dimensionality spectral channels, and designing effective CD algorithms (especially the unsupervised and automatic ones). By now, almost all existing CD approaches focus mainly on the spectral domain, analyzing in detail the changes in HS images from the spectral variation point of view. In future research, more attention should be paid to jointly analyzing the spatial information and the temporal correlation information to improve the performance of current CD techniques. This could be done by introducing techniques to consider spatial correlation, such as Markov random fields or a convolutional neural network based on deep learning.

CD in image time series is currently conducted mainly on MS images. The availability of HS sensors on different spaceborne platforms will likely lead to a decrease in the revisit time over a given area, thus improving temporal resolution. This will lead to more and more HS time series consisting of tens of images. In this case, existing time series algorithms will not be sufficient to effectively handle the enormous number of big HS data to extract all relevant information. Therefore, new ad hoc methods capable of handling the HS-temporal dimension will be required. Furthermore, current CD methods for image time series focus mainly on binary problems or a specific change class (e.g., vegetation). The design of new advanced techniques that can accurately detect multiclass changes is an important future research direction.

A platform that is becoming relevant for HS acquisitions is based on unmanned autonomous vehicles (UAVs). Currently, there is an increasing number of HS sensors designed specifically to be mounted on UAVs. UAVs allow for on-demand acquisitions after relevant events and also for periodic acquisitions that can be used in different multitemporal applications. The most important difference between HS sensors mounted on UAVs and those mounted on satellites is the possibility of acquiring data at extremely high spatial resolution. This requires a redefinition of the concept of *change* because, when working at such a high resolution, it is possible to detect

changes caused by very subtle spectral variations in the analyzed scene (e.g., variation in foliage characteristics, even at the level of single branches in a tree). Therefore, it will be important to understand what the changes of interest are for a given application and how to discriminate them among the other subtle changes. The high resolution and instability of UAV platforms will also require ad hoc preprocessing operations to have high-quality data for the CD steps. This includes accurate georeferencing and registration algorithms able to reduce the impact of georeferencing errors during the acquisition process. As a final remark, it will be especially relevant to define a multitemporal HS image benchmark with reference data to be used for the quantitative validation of available and future CD techniques.

**NEW AD HOC METHODS
CAPABLE OF HANDLING THE
HS-TEMPORAL DIMENSION
WILL BE REQUIRED.**

ACKNOWLEDGMENTS

This work was partly supported by the Natural Science Foundation of China (41601354), the Fundamental Research Funds for the Central Universities (22120180005), and the University of Trento, Italy.

AUTHOR INFORMATION

Sicong Liu (sicong.liu@tongji.edu.cn) received his B.Sc. degree in geographical information systems and his M.E. degree in photogrammetry and remote sensing from China University of Mining and Technology, in 2009 and 2011, respectively. He received his Ph.D. degree in information and communication technology from the University of Trento, Italy, in 2015. Currently, he is with the College of Surveying and Geoinformatics, Tongji University, Shanghai, China. He is a Member of the IEEE.

Daniele Marinelli (daniele.marinelli@unitn.it) received his B.Sc. degree in electronics and telecommunications engineering and his M.Sc. degree in telecommunications engineering (summa cum laude) from the University of Trento, Italy, in 2013 and 2015, respectively. Currently, he is with the Department of Information Engineering and Computer Science, University of Trento. He is a Student Member of the IEEE.

Lorenzo Bruzzone (lorenzo.bruzzone@unitn.it) received his M.S. degree in electronic engineering (summa cum laude) and his Ph.D. degree in telecommunications from the University of Genoa, Italy, in 1993 and 1998, respectively. Currently, he is with the Department of Information Engineering and Computer Science, University of Trento, Italy. He is a Fellow of the IEEE.

Francesca Bovolo (bovolo@fbl.eu) received her B.S. and M.S. (summa cum laude) degrees in telecommunication engineering, and her Ph.D. degree in communication and information technologies from the University of Trento, Italy, in 2001, 2003, and 2006, respectively. Currently,

she is with the Fondazione Bruno Kessler, Center for Information and Communication Technology, Trento. She is a Senior Member of the IEEE.

REFERENCES

- [1] F. Bovolo and L. Bruzzone, "The time variable in data fusion: A change detection perspective," *IEEE Geosci. Remote Sens. Mag.*, vol. 3, no. 3, pp. 8–26, Sept. 2015. doi: 10.1109/MGRS.2015.2443494.
- [2] M. A. Cutter, D. R. Lobb, and R. A. Cockshott, "Compact high resolution imaging spectrometer (CHRIS)," *Acta Astronautica*, vol. 46, no. 2, pp. 263– 268, 2000. doi: 10.1016/S0094-5765(99)00207-6.
- [3] X. Gu and X. Tong, "Overview of china earth observation satellite programs [space agencies]," *IEEE Geosci. Remote Sens. Mag.*, vol. 3, no. 3, pp. 113–129, Sept. 2015.
- [4] A. Kumar, A. Saha, and V. K. Dadhwal, "Some issues related with sub-pixel classification using HYSI data from IMS-1 satellite," *J. Indian Soc. Remote Sens.*, vol. 38, no. 2, pp. 203–210, June 2010. doi: 10.1007/s12524-010-0027-5.
- [5] L. Candela, R. Formaro, R. Guarini, R. Loizzo, F. Longo, and G. Varacalli, "The PRISMA mission," in *Proc. 2016 IEEE Int. Geoscience and Remote Sensing Symp. (IGARSS)*, July 2016, pp. 253–256.
- [6] T. Matsunaga et al., "Current status of hyperspectral imager suite (HISUI) onboard international space station (ISS)," in *Proc. 2017 IEEE Int. Geoscience and Remote Sensing Symp. (IGARSS)*, July 2017, pp. 443–446.
- [7] L. Guanter et al., "The EnMAP spaceborne imaging spectroscopy mission for earth observation," *Remote Sens.*, vol. 7, no. 7, pp. 8830–8857, 2015. doi: 10.3390/rs70708830.
- [8] C. M. Lee et al., "An introduction to the NASA Hyperspectral Infrared Imager (HypIRI) mission and preparatory activities," *Remote Sens. Environ.*, vol. 167, pp. 6– 19, 2015. doi: 10.1016/j.rse.2015.06.012.
- [9] T. Feingersh and E. B. Dor, "SHALOM: A commercial hyperspectral space mission," in *Optical Payloads for Space Missions*, S.-E. Qian, Ed. Hoboken, NJ: Wiley, 2015, pp. 247–263.
- [10] J. Transon, R. d'Andrimont, A. Maugnard, and P. Defourny, "Survey of hyperspectral earth observation applications from space in the sentinel-2 context," *Remote Sens.*, vol. 10, no. 2, pp. 157, 2018. doi: 10.3390/rs10020157.
- [11] P. Ghamisi et al., "Advances in hyperspectral image and signal processing: A comprehensive overview of the state of the art," *IEEE Geosci. Remote Sens. Mag.*, vol. 5, no. 4, pp. 37–78, Dec. 2017. doi: 10.1109/MGRS.2017.2762087.
- [12] P. Du, S. Liu, L. Bruzzone, and F. Bovolo, "Target-driven change detection based on data transformation and similarity measures," in *Proc. 2012 IEEE Int. Geoscience and Remote Sensing Symp.*, July 2012, pp. 2016–2019.
- [13] P. Coppin, I. Jonckheere, K. Nackaerts, B. Muys, and E. Lambin, "Digital change detection methods in ecosystem monitoring: A review," *Int. J. Remote Sens.*, vol. 25, no. 9, pp. 1565–1596, 2004. doi: 10.1080/0143116031000101675.
- [14] S. Liu, M. Chi, Y. Zou, A. Samat, J. A. Benediktsson, and A. Plaza, "Oil spill detection via multitemporal optical remote sensing images: A change detection perspective," *IEEE Geosci. Remote Sens. Lett.*, vol. 14, no. 3, pp. 324–328, 2017. doi: 10.1109/LGRS.2016.2639540.
- [15] F. Bovolo and L. Bruzzone, "A split-based approach to unsupervised change detection in large-size multitemporal images: Application to tsunami-damage assessment," *IEEE Trans. Geosci. Remote Sens.*, vol. 45, no. 6, pp. 1658–1670, 2007. doi: 10.1109/TGRS.2007.895835.
- [16] P. Du, S. Liu, P. Gamba, and K. Tan, "Fusion of difference images for change detection over urban areas," *IEEE J. Sel. Topics Appl. Earth Observ. Remote Sens.*, vol. 5, no. 4, pp. 1076–1086, Aug. 2012. doi: 10.1109/JSTARS.2012.2200879.
- [17] J. L. R. X. Huang and D. Wen, "Multi-level monitoring of subtle urban changes for the megacities of China using high-resolution multi-view satellite imagery," *Remote Sens. Environ.*, vol. 56, pp. 56–75, 2017. doi: 10.1016/j.rse.2017.05.001.
- [18] L. Z. Dawei Wen, X. Huang, and J. A. Benediktsson, "A novel automatic change detection method for urban high-resolution remotely sensed imagery based on multiindex scene representation," *IEEE Trans. Geosci. Remote Sens.*, vol. 54, no. 1, pp. 609–625, 2015.
- [19] D. Lu, P. Mausel, E. Brondizio, and E. Moran, "Change detection techniques," *Int. J. Remote Sens.*, vol. 25, no. 12, pp. 2365–2401, 2004. doi: 10.1080/0143116031000139863.
- [20] D. Lu, G. Li, and E. Moran, "Current situation and needs of change detection techniques," *Int. J. Image Data Fusion*, vol. 5, no. 1, pp. 13–38, 2014. doi: 10.1080/19479832.2013.868372.
- [21] Y. Ban and O. Yousif, "Change detection techniques: A review" in *Multitemporal Remote Sensing: Methods and Applications*, Y. Ban, Ed. New York: Springer-Verlag, 2016, pp. 19–43.
- [22] L. Bruzzone, S. Liu, F. Bovolo, and P. Du, "Change detection in multitemporal hyperspectral images," in *Multitemporal Remote Sensing: Methods and Applications*, Y. Ban, Ed. New York: Springer-Verlag, 2016, pp. 63–88.
- [23] M. Hasanlou and S. T. Seydi, "Hyperspectral change detection: An experimental comparative study," *Int. J. Remote Sens.*, vol. 39, no. 20, pp. 7029–7083, 2018.
- [24] T. Doggett and N. Memarsadeghi, "NASA computational case study, hyperspectral data processing: Cryospheric change detection," *Computing Sci. Eng.*, vol. 14, no. 4, pp. 92–97, July 2012. doi: 10.1109/MCSE.2012.43.
- [25] S. Liu, "Advanced techniques for automatic change detection in multitemporal hyperspectral images," Ph.D. thesis, Dept. Inform. Eng. Comput. Sci., Univ. of Trento, Italy, 2015.
- [26] A. Singh, "Review article digital change detection techniques using remotely-sensed data," *Int. J. Remote Sens.*, vol. 10, no. 6, pp. 989–1003, 1989. doi: 10.1080/01431168908903939.
- [27] F. Bovolo, S. Marchesi, and L. Bruzzone, "A framework for automatic and unsupervised detection of multiple changes in multitemporal images," *IEEE Trans. Geosci. Remote Sens.*, vol. 50, no. 6, pp. 2196–2212, June 2012. doi: 10.1109/TGRS.2011.2171493.
- [28] S. Liu, Q. Du, X. Tong, A. Samat, H. Pan, and X. Ma, "Band selection-based dimensionality reduction for change detection in multi-temporal hyperspectral images," *Remote Sens.*, vol. 9, no. 10, pp. 1–23, 2017.
- [29] D. Haboudane, J. R. Miller, E. Pattey, P. J. Zarco-Tejada, and I. B. Strachan, "Hyperspectral vegetation indices and novel algorithms for predicting green lai of crop canopies: Modeling and validation in the context of precision agriculture," *Remote*

- Sens. Environ.*, vol. 90, no. 3, pp. 337–352, 2004. doi: 10.1016/j.rse.2003.12.013.
- [30] R. D. Johnson and E. S. Kasischke, “Change vector analysis: A technique for the multispectral monitoring of land cover and condition,” *Int. J. Remote Sens.*, vol. 19, no. 3, pp. 411–426, 1998. doi: 10.1080/014311698216062.
- [31] F. Bovolo and L. Bruzzone, “A theoretical framework for unsupervised change detection based on change vector analysis in the polar domain,” *IEEE Trans. Geosci. Remote Sens.*, vol. 45, no. 1, pp. 218–236, Jan. 2007. doi: 10.1109/TGRS.2006.885408.
- [32] J. Chen, X. Chen, X. Cui, and J. Chen, “Change vector analysis in posterior probability space: A new method for land cover change detection,” *IEEE Geosci. Remote Sens. Lett.*, vol. 8, no. 2, pp. 317–321, Mar. 2011. doi: 10.1109/LGRS.2010.2068537.
- [33] L. Bruzzone and S. B. Serpico, “An iterative technique for the detection of land-cover transitions in multitemporal remote-sensing images,” *IEEE Trans. Geosci. Remote Sens.*, vol. 35, no. 4, pp. 858–867, July 1997. doi: 10.1109/36.602528.
- [34] L. Bruzzone, D. F. Prieto, and S. B. Serpico, “A neural-statistical approach to multitemporal and multisource remote-sensing image classification,” *IEEE Trans. Geosci. Remote Sens.*, vol. 37, no. 3, pp. 1350–1359, May 1999. doi: 10.1109/36.763299.
- [35] S. Liu, L. Bruzzone, F. Bovolo, and P. Du, “Hierarchical unsupervised change detection in multitemporal hyperspectral images,” *IEEE Trans. Geosci. Remote Sens.*, vol. 53, no. 1, pp. 244–260, Jan. 2015.
- [36] S. Liu, L. Bruzzone, F. Bovolo, and M. Zanetti, “Sequential spectral change vector analysis for iteratively discovering and detecting multiple changes in hyperspectral images,” *IEEE Trans. Geosci. Remote Sens.*, vol. 53, no. 8, pp. 4363–4378, 2015. doi: 10.1109/TGRS.2015.2396686.
- [37] S. Liu, X. Tong, L. Bruzzone, and P. Du, “A novel semisupervised framework for multiple change detection in hyperspectral images,” in *Proc. 2017 IEEE Int. Geoscience and Remote Sensing Symp. (IGARSS)*, July 2017, pp. 173–176.
- [38] S. Liu, L. Bruzzone, F. Bovolo, and P. Du, “Unsupervised multitemporal spectral unmixing for detecting multiple changes in hyperspectral images,” *IEEE Trans. Geosci. Remote Sens.*, vol. 54, no. 5, pp. 1–16, 2016.
- [39] A. Ertürk and A. Plaza, “Informative change detection by unmixing for hyperspectral images,” *IEEE Geosci. Remote Sens. Lett.*, vol. 12, no. 6, pp. 1252–1256, 2015. doi: 10.1109/LGRS.2015.2390973.
- [40] L. Bruzzone and D. Fernandezprieto, “A minimum-cost thresholding technique for unsupervised change detection,” *Int. J. Remote Sens.*, vol. 21, no. 18, pp. 3539–3544, 2000. doi: 10.1080/014311600750037552.
- [41] L. Bruzzone and D. F. Prieto, “Automatic analysis of the difference image for unsupervised change detection,” *IEEE Trans. Geosci. Remote Sens.*, vol. 38, no. 3, pp. 1171–1182, 2000. doi: 10.1109/36.843009.
- [42] B.-C. Gao and A. F. H. Goetz, “Column atmospheric water vapor and vegetation liquid water retrievals from airborne imaging spectrometer data,” *J. Geophys. Res. Atmospheres*, vol. 95, no. D4, pp. 3549–3564, 1990. doi: 10.1029/JD095iD04p03549.
- [43] S. M. Adler-Golden et al., “Atmospheric correction for short-wave spectral imagery based on MODTRAN4,” *Proc. SPIE-Int. Soc. Opt. Eng.*, vol. 3753, pp. 3753–3753, 1999. doi: 10.1117/12.366315.
- [44] M. Dalponte, L. Bruzzone, L. Vescovo, and D. Gianelle, “The role of spectral resolution and classifier complexity in the analysis of hyperspectral images of forest areas,” *Remote Sens. Environ.*, vol. 113, no. 11, pp. 2345–2355, 2009. doi: 10.1016/j.rse.2009.06.013.
- [45] A. Schaum and A. Stocker, “Long-interval chronochrome target detection,” in *Proc. 1997 Int. Symp. Spectral Sensing Research*, 1998, pp. 1760–1770.
- [46] A. P. Schaum and A. Stocker, “Hyperspectral change detection and supervised matched filtering based on covariance equalization,” *Proc. SPIE-Int. Soc. Opt. Eng.*, vol. 5425, pp. 77–90, 2004.
- [47] M. Shimoni, R. Heremans, and C. Perneel, “Detection of small changes in complex urban and industrial scenes using imaging spectroscopy,” in *Proc. 2010 IEEE Int. Geoscience and Remote Sensing Symp.*, July 2010, pp. 4757–4760.
- [48] J. Theiler, C. Scovel, B. Wohlberg, and B. R. Foy, “Elliptically contoured distributions for anomalous change detection in hyperspectral imagery,” *IEEE Geosci. Remote Sens. Lett.*, vol. 7, no. 2, pp. 271–275, Apr. 2010. doi: 10.1109/LGRS.2009.2032565.
- [49] N. Acito, M. Diani, G. Corsini, and S. Resta, “Introductory view of anomalous change detection in hyperspectral images within a theoretical Gaussian framework,” *IEEE Aerospace Electron. Syst. Mag.*, vol. 32, no. 7, pp. 2–27, 2017. doi: 10.1109/MAES.2017.160155.
- [50] C. Wu, L. Zhang, and B. Du, “Hyperspectral anomaly change detection with slow feature analysis,” *Neurocomputing*, vol. 151, pp. 175–187, 2015. doi: 10.1016/j.neucom.2014.09.058.
- [51] J. Zhou, C. Kwan, B. Ayhan, and M. T. Eismann, “A novel cluster kernel RX algorithm for anomaly and change detection using hyperspectral images,” *IEEE Trans. Geosci. Remote Sens.*, vol. 54, no. 11, pp. 6497–6504, 2016. doi: 10.1109/TGRS.2016.2585495.
- [52] J. Meola, M. T. Eismann, R. L. Moses, and J. N. Ash, “Application of model-based change detection to airborne VNIR/SWIR hyperspectral imagery,” *IEEE Trans. Geosci. Remote Sens.*, vol. 50, no. 10, pp. 3693–3706, 2012. doi: 10.1109/TGRS.2012.2186305.
- [53] J. Theiler and B. Wohlberg, “Local coregistration adjustment for anomalous change detection,” *IEEE Trans. Geosci. Remote Sens.*, vol. 50, no. 8, pp. 3107–3116, 2012. doi: 10.1109/TGRS.2011.2179942.
- [54] K. Vongsy, M. J. Mendenhall, M. T. Eismann, and G. L. Peterson, “Removing parallax-induced changes in hyperspectral change detection,” in *Proc. 2012 IEEE Int. Geoscience and Remote Sensing Symp.*, 2012, pp. 2012–2015.
- [55] J. Meola, M. T. Eismann, K. J. Barnard, and R. C. Hardie, “Analysis of hyperspectral change detection as affected by vegetation and illumination variations,” *Proc. SPIE-Int. Soc. Opt. Eng.*, pp. 65651S–65651S, 2007. doi: 10.1117/12.716324.
- [56] J. Meola and M. T. Eismann, “Image misregistration effects on hyperspectral change detection,” *Proc. SPIE-Int. Soc. Opt. Eng.*, vol. 6966, 2008, p. 69660Y. doi: 10.1117/12.775434.
- [57] M. T. Eismann, J. Meola, and R. C. Hardie, “Hyperspectral change detection in the presence of diurnal and seasonal variations,”

- IEEE Trans. Geosci. Remote Sens.*, vol. 46, no. 1, pp. 237–249, 2008. doi: 10.1109/TGRS.2007.907973.
- [58] M. Frank and M. Canty, “Unsupervised change detection for hyperspectral images,” in *Proc. AVIRIS Workshop*, 2003, pp. 63–72.
- [59] A. A. Nielsen, “The regularized iteratively reweighted mad method for change detection in multi- and hyperspectral data,” *IEEE Trans. Image Process.*, vol. 16, no. 2, pp. 463–478, 2007. doi: 10.1109/TIP.2006.888195.
- [60] A. A. Nielsen, “Kernel maximum autocorrelation factor and minimum noise fraction transformations,” *IEEE Trans. Image Process.*, vol. 20, no. 3, pp. 612–624, 2011.
- [61] V. Ortiz-Rivera, M. Vélez-Reyes, and B. Roysam, “Change detection in hyperspectral imagery using temporal principal components,” *Proc. SPIE-Int. Soc. Opt. Eng.*, vol. 6233, 2006. doi: 10.1117/12.667961.
- [62] S. Hemissi, I. R. Farah, K. S. Ettabaa, and B. Solaiman, “A new spatio-temporal ICA for multi-temporal endmembers extraction and change trajectory analysis,” in *Piers Marrakesh Progress in Electromagnetics Research Symp.*, 2011, pp. 1289–1293.
- [63] S. Liu, L. Bruzzone, F. Bovolo, and P. Du, “Unsupervised hierarchical spectral analysis for change detection in hyperspectral images,” in *Proc. 2012 4th Workshop Hyperspectral Image and Signal Processing (WHISPERS)*, 2012. doi: 10.1109/WHISPERS.2012.6874245.
- [64] C. Wu, B. Du, and L. Zhang, “A subspace-based change detection method for hyperspectral images,” *IEEE J. Sel. Topics Appl. Earth Observ. Remote Sens.*, vol. 6, no. 2, pp. 815–830, 2013. doi: 10.1109/JSTARS.2013.2241396.
- [65] Q. Du, L. Wasson, and R. King, “Unsupervised linear unmixing for change detection in multitemporal airborne hyperspectral imagery,” in *Proc. 2005 Int. Workshop Analysis of Multi-Temporal Remote Sensing Images*, 2005, pp. 136–140.
- [66] A. Ertürk, M. D. Iordache, and A. Plaza, “Sparse unmixing-based change detection for multitemporal hyperspectral images,” *IEEE J. Sel. Topics Appl. Earth Observ. Remote Sens.*, vol. 9, no. 2, pp. 708–719, 2015. doi: 10.1109/JSTARS.2015.2477431.
- [67] A. Ertürk, M. D. Iordache, and A. Plaza, “Sparse unmixing with dictionary pruning for hyperspectral change detection,” *IEEE J. Sel. Topics Appl. Earth Observ. Remote Sens.*, vol. 10, no. 1, pp. 321–330, Jan. 2017.
- [68] Y. Yuan, H. Lv, and X. Lu, “Semi-supervised change detection method for multi-temporal hyperspectral images,” *Neurocomputing*, vol. 148, pp. 363–375, 2015. doi: 10.1016/j.neucom.2014.06.024.
- [69] Q. Du, N. Younan, and R. King, “Change analysis for hyperspectral imagery,” in *Int. Workshop Analysis of Multi-temporal Remote Sensing Images*, 2007. doi: 10.1109/MULTITEMP.2007.4293052.
- [70] Z. Chen and B. Wang, “Spectrally-spatially regularized low-rank and sparse decomposition: A novel method for change detection in multitemporal hyperspectral images,” *Remote Sens.*, vol. 9, no. 10, pp. 1–21, 2017.
- [71] D. Marinelli, F. Bovolo, and L. Bruzzone, “A novel change detection method for multitemporal hyperspectral images based on binary hyperspectral change vectors,” *IEEE Trans. Geosci. Remote Sens.*, 2019. doi: 10.1109/TGRS.2019.2894339.
- [72] J. Yang and W. Sun, “Automatic analysis of the slight change image for unsupervised change detection,” *J. Appl. Remote Sens.*, vol. 9, no. 1, p. 095995, 2015. doi: 10.1117/1.JRS.9.095995.
- [73] S. Hemissi, I. R. Farah, K. S. Ettabaa, and B. Solaiman, “Multi-spectro-temporal analysis of hyperspectral imagery based on 3-D spectral modeling and multilinear algebra,” *IEEE Trans. Geosci. Remote Sens.*, vol. 51, no. 1, pp. 199–216, 2013. doi: 10.1109/TGRS.2012.2200486.
- [74] S. Henrot, J. Chanussot, and C. Jutten, “Dynamical spectral unmixing of multitemporal hyperspectral images,” *IEEE Trans. Image Process.*, vol. 25, no. 9, pp. 4443–4443, 2016.
- [75] M. A. Veganzones, J. E. Cohen, R. C. Farias, J. Chanussot, and P. Comon, “Nonnegative tensor CP decomposition of hyperspectral data,” *IEEE Trans. Geosci. Remote Sens.*, vol. 54, no. 5, pp. 2577–2588, 2016. doi: 10.1109/TGRS.2015.2503737.
- [76] M. T. Eismann and J. Meola, “Hyperspectral change detection: Methodology and challenges,” in *Proc. IGARSS 2008–2008 IEEE Int. Geoscience and Remote Sensing Symp.*, 2008, pp. II-605–II-608.
- [77] K. Vongsy and M. J. Mendenhall, “A comparative study of spectral detectors,” in *3rd Workshop on Hyperspectral Image and Signal Processing: Evolution in Remote Sensing (WHISPERS)*, June 2011, pp. 1–4.
- [78] Y. Du, C. Chang, H. Ren, C. C. Chang, and F. M. D’Amico, “New hyperspectral discrimination measure for spectral characterization,” *Opt. Eng.*, vol. 43, no. 8, pp. 1777–1786, 2004. doi: 10.1117/1.1766301.
- [79] M. Zanetti, F. Bovolo, and L. Bruzzone, “Rayleigh-rice mixture parameter estimation via EM algorithm for change detection in multispectral images,” *IEEE Trans. Image Process.*, vol. 24, no. 12, pp. 5004–5016, 2015. doi: 10.1109/TIP.2015.2474710.
- [80] A. A. Nielsen, K. Conradsen, and J. J. Simpson, “Multivariate alteration detection (MAD) and MAF postprocessing in multispectral, bitemporal image data: New approaches to change detection studies,” *Remote Sens. Environ.*, vol. 64, no. 1, pp. 1–19, 1998. doi: 10.1016/S0034-4257(97)00162-4.
- [81] N. Otsu, “A threshold selection method from gray-level histograms,” *IEEE Trans. Syst., Man, Cybern.*, vol. 9, no. 1, pp. 62–66, Jan. 1979. doi: 10.1109/TSMC.1979.4310076.
- [82] B. Jeon and D. A. Landgrebe, “Classification with spatio-temporal interpixel class dependency contexts,” *IEEE Trans. Geosci. Remote Sens.*, vol. 30, no. 4, pp. 663–672, July 1992. doi: 10.1109/36.158859.
- [83] X. L. Dal and S. Khorram, “Remotely sensed change detection based on artificial neural networks,” *Photogrammetric Eng. Remote Sens.*, vol. 65, no. 10, pp. 1187–1194, 1999.
- [84] P. Du, S. Liu, P. Liu, K. Tan, and L. Cheng, “Sub-pixel change detection for urban land-cover analysis via multi-temporal remote sensing images,” *Geospatial Inform. Sci.*, vol. 17, no. 1, pp. 26–38, 2014. doi: 10.1080/10095020.2014.889268.
- [85] Redazione ASI. “PRISMA satellite successful launched,” Agenzia Spaziale Italiana. [Online]. Available: <https://www.asi.it/en/news/prisma-satellite-successful-launched>